J. Serb. Chem. Soc. 72 (6) 563–578 (2007) UDC 546.76+546.226–325:548.7:544.6:620.193
JSCS–3588 *Original scientific paper*

Structural effects of metallic chromium on its electrochemical behavior

BORE JEGDIĆ[1], DRAGUTIN M. DRAŽIĆ[2*#], JOVAN P. POPIĆ[2#] and VELIMIR RADMILOVIĆ[3]

[1]*Institute for Chemical Power Sources, Batajnički drum bb. 11070 Belgrade-Zemun,* [2]*Institute of Chemistry, Technology and Metallurgy-Center for Electrochemistry, P. O. Box 473, 11001 Belgrade, Serbia and* [3]*Lawrence Berkley National Laboratories, University of California, Berkeley, CA, USA (e-mail: dmdrazic@eunet.yu)*

(Received 20 February 2007)

Abstract: Chromium dissolution in aqueous sulfuric acid solution of pH 1 was studied electrochemically on chromium electrodes with different crystallographic structures. A slow potentiodynamic method was used for the electrochemical measurements in deaerated solutions (purged with nitrogen), while the Cr(III) ions in the solution after the corrosion were determined by atomic absorption spectrometry. Three electrode materials with a very dominant crystallite orientation resembling single crystal structures (*i.e.*, 111 and 110) confirmed by the electron backscattering diffraction (EBSD), were used in the experiments. The (111) structures were somewhat more active electrochemically (both anodic and cathodic) than the (110) structure. However, Cr electrochemically deposited in standard plating bath, assumed from literature data to has also the (111) structure, was more than 4 times active for anodic dissolution and, by the same number, less active for cathodic hydrogen evolution. The concentrations of Cr(III) ions determined in the solution after definite times of corrosion of all the materials showed almost two times larger dissolution rates than observed electrochemically by three different electrochemical methods (Wagner–Traud, Stern–Geary, electrochemical impedance spectroscopy). This is explained by the simultaneous occurrence of potential independent chemical dissolution of Cr, by a direct reaction of metallic Cr with H_2O molecules, proposed a long time ago by Kolotyrkin and coworkers.

Keywords: chromium, crystalline structure, electrochemistry, corrosion, sulfuric acid.

INTRODUCTION

It was shown in previous works[1–4] that metallic chromium in deaerated sulfuric acid dissolves by two different mechanisms. One is the electrochemical mechanism involved in the electrochemical corrosion of metals in acid solutions, which follows the Wagner–Traud,[5] interpretation of the acid corrosion processes and the

* Author for correspondence.
# Serbian Chemical Society member.

doi: 10.2298/JSC0706563J

second one, the chemical model of Kolotyrkin *et al.*[6–12] in which the metal dissolution reaction proceeds in the form of a chemical reaction by direct reaction of metal atoms with water molecules, with a possible participation of hydronium ions. In these processes there are no electron transfer reaction steps through the double layer and, therefore, these reactions do not depend on the electrode potential, contrary to those which involve electron transfer, *e.g.,* electrochemical anodic dissolution. In the reported experimental results it was shown that the rates of these reactions depend to some extent, on the crystallographic orientation of the crystallites in the electrode material.[4] This finding was made accidentally, since by chance the metallic chromium used in these experiments was a cast large grain specimen. Hence grains as large as 5 mm in diameter could be analyzed.

In the work presented here, the influence of the crystallographic structure of the surface on electrochemical and chemical dissolution in sulfuric acid was studied by comparing these properties for three metallic chromium samples obtained by three different methods of preparation; casting, rolling and by electrochemical deposition from a standard chromium plating bath.

EXPERIMENTAL

The experiments were performed with metallic chromium (Merck, cast, lumps), marked A, metalic Cr (Goodfellow, Berwin, Pa, USA), as 5 mm rods marked B, and electroplated Cr on steel coupons *ca*. 120 μm thick, marked C.

Electrode A. These electrodes consisted of the Merck chromium sealed in an acrylic resin in the form of a piece of metal with an exposed surface of 1 cm^2. The electrode surface was mechanically polished stepwise using finally polishing paper of the quality 0. Such surfaces were etched in the sulfuric acid solution used in the experiments. The etching revealed that the chromium surface consisted of two or three large crystal surfaces, indicating that Merck chromium is composed of large macro crystals, probably formed during the slow cooling during the casting process. Figure 1a represents a photograph of an electrode A after polishing the diameter of the whole electrode is *ca*. 2 cm, and a microphotograph after anodic dissolution for *ca*. 60 min (×150) , with one boundary between two large grains. Such electrodes were electrochemically studied either as one complex entity, or the parts representing only one grain left unprotected while the rest of the surface was protected by acrylic resin. Hence, a single grain could be electrochemically studied alone. Such surfaces were marked as electrode A1 and A2.

Electrode A1. The numbers in Fig. 1a designate the surfaces corresponding to the grains A1 and A2. The estimated surface area of grain 1 was 0.5 cm^2, while the crystallographic orientation of the grain is presented later in the text.

Electrode A2. The surface area of grain 2 was estimated to be 0.35 cm^2. The crystallographic orientation of grain 2 is presented later in the text.

The results reported in this work are related to electrodes A, A1 and A2 as defined above, since the crystal orientation was determined for these two specific surfaces, *i.e.*, A1 and A2.

Electron B. Chromium rod 5.0 mm in diameter (Goodfellow, Berwin, Pa, USA, 99.8 %) was sealed in acrylic resin and cut perpendicularly so that only a disk of the surface area, estimated to be 0.2 cm^2 was exposed to the solution. The estimate of the crystallilne structure of these electrodes is presented later in the text. The microphotograph of surface B after *ca*. 60 min of polarization is shown in Fig. 1b.

Electrode C. These electrodes were made of mild steel coupons electrolytically covered with a *ca.* 120 μm thick chromium deposit. For plating, a standard procedure for Cr plating bath was used (235 g/dm^3 CrO_3, 4.5 g/dm^3 Cr_2O_3, 2.67 g/dm^3 H_2SO_4, j = 55 A/ dm^2, t = 55 °C). Microphotographs

of surfaces of the electrode C, before etching and after 60 min of polarization measurements are presented in Fig. 1c, (1) and (2), respectively.

All the experiments were performed in aqueous mixtures of 0.1 M $NaSO_4$ + H_2SO_4, the concentrations of the acid being adjusted so to give that pH of 1.0. Merck p.a. chemicals and doubly distilled water were used for the preparation of the solutions. An all glass thermostated three compartment electrochemical cell with a platinum foil as the counter electrode and a saturated calomel reference electrode (SCE) were used. All the potentials are referred to the SCE. The solution were continuously deaerated with purified nitrogen. The experiments were carried out at 25±0.2 °C). The electrical measurements were performed with a PAR 273 potentiostat–galvanostat set up, Houston X–Y recorder and 5315 lock-in-amplifier for the electrochemical spectroscopy measurements, using 332 Corrosion Software and 368 AC-Impedance Software.

When the chromium electrode after polishing in air was introduced into the solution, even after purging the solution with purified N_2 the spontaneously established open circuit potential, $E_{corr,1}$, was about –0.450 V in pH 1.0, which corresponds to the potential of a passivated electrode. Prior to the measurements, the chromium electrodes were activated by cathodic polarization at –0.9 V for 90 s to reduce the thin oxide film formed at the surface while the electrode was in contact with air. After 15 min stabilization at the corrosion potential, polarization curves were recorded starting from the corrosion potential in cathodic and anodic direction with a sweep rate of 2 mV/s. This sweep rate appeared to be sufficiently slow to consider the polarization curves to have been obtained under a quasi steady state condition. Of course, this does not hold for the passive range of the anodic curve, since the passive current permanently decreases over time.

Chemical analysis of the solution for determining the concentration of the total dissolved chromium as Cr(III) was made by atomic adsorption spectroscopy (Perkin Elmer 1100). Since in a previous work,[1] it was shown that some of the chromium dissolves as Cr(II) and some as Cr(III) in the ratio 1:7, the equivalent metallic chromium dissolution rate was calculated from the Cr(III) concentration using the apparent valence $n = 2.12$ for Cr.

Structural analysis of the electrode materials

The electron backscattering diffraction (EBSD) technique was employed to determine the local textures as well as the grain size and distributions of the misorientation angles using OIM (color coded pictures based on inverse pole figures). The experimental data were collected using a DB-235 FEI® FIB equipped with a TSL® orientation imaging system at the National Center for Electron Microscopy, Lawrence Berkeley National Laboratory.

RESULTS

Electrode structure

The microphotographs presented in Fig. 1 clearly show that electrodes A, B and C have different crystallographic structures and textures, which enabled the effect of the electrode structure on its electrochemical and chemical behavior to be investigated. The crystallographic examination revealed that electrode A had two separated macro grains, appearing as two single crystal structures. These results will be presented in the following text.

Electrode A1. X-Ray analysis did not show a Laueogram as expected from a single crystal structure.[4] However, texture analysis showed that this grain is a monocrystal, but consisting of domains of different orientation, predominantly (111), as shown in Fig. 2a., which represent the inverse pole figure obtained by Electron Backscattering Difraction analysis (EBSD). Therefore, this texture could be considered further as a structure (111) crystal orientation.

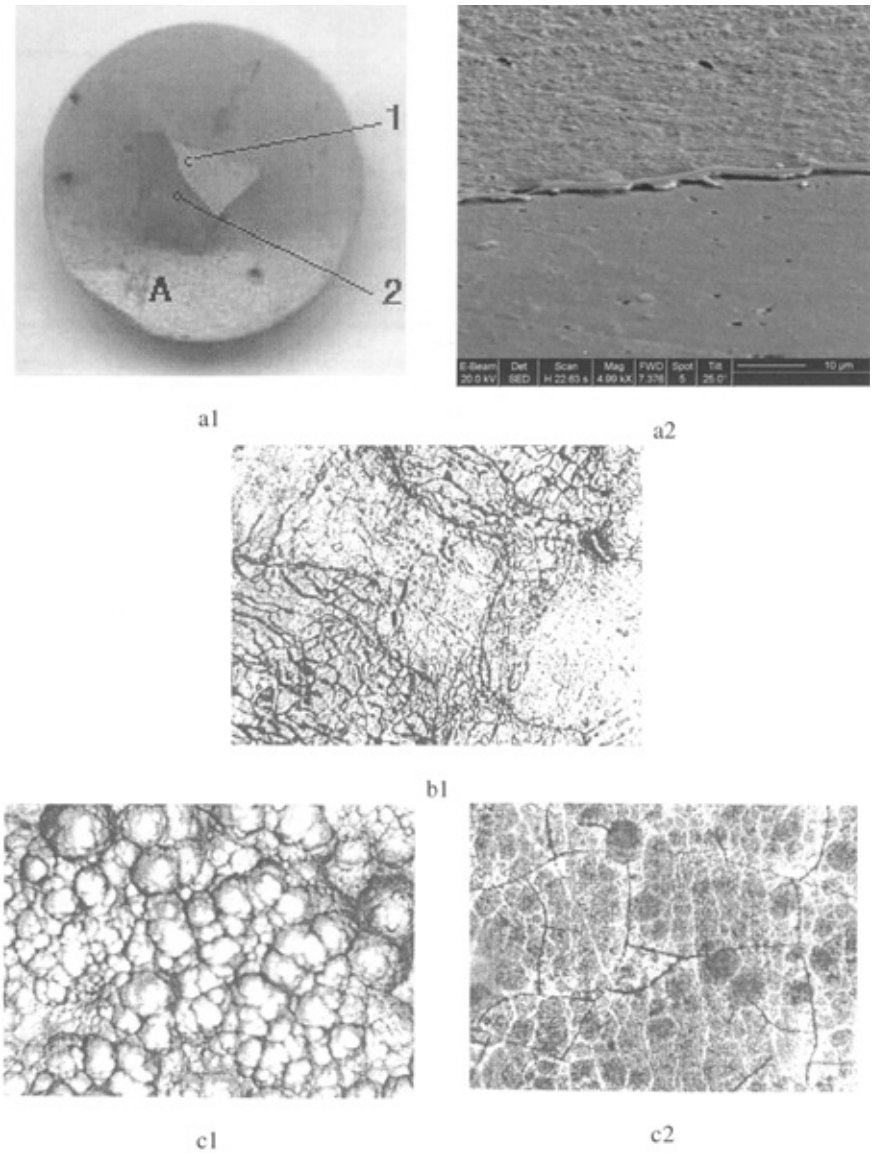

Fig. 1. (al) – Photograph of electrode A with the resin holder (total diameter 2 cm); (a2) – SEM of the grain boundary region between the surfaces of the electrodes A1 (111) and A2(110); (b) – Microphotograph of electrode B after etching for 15 min in the studied solution (×500); (cl) – Microphotography of the electrode C before electrochemical treatment (×500): (c2) – surface of the electrode C after the electrochemical treatment for 60 min (×500).

Electrode A2. The texture analysis of this surface, as shown in Fig. 2b, indicates a dominant (110) structure, *i.e.,* grain 2 could be considered as a single crystal of the orientation (110), which is a more packed surface of the bcc Cr lattice then the (111) one.

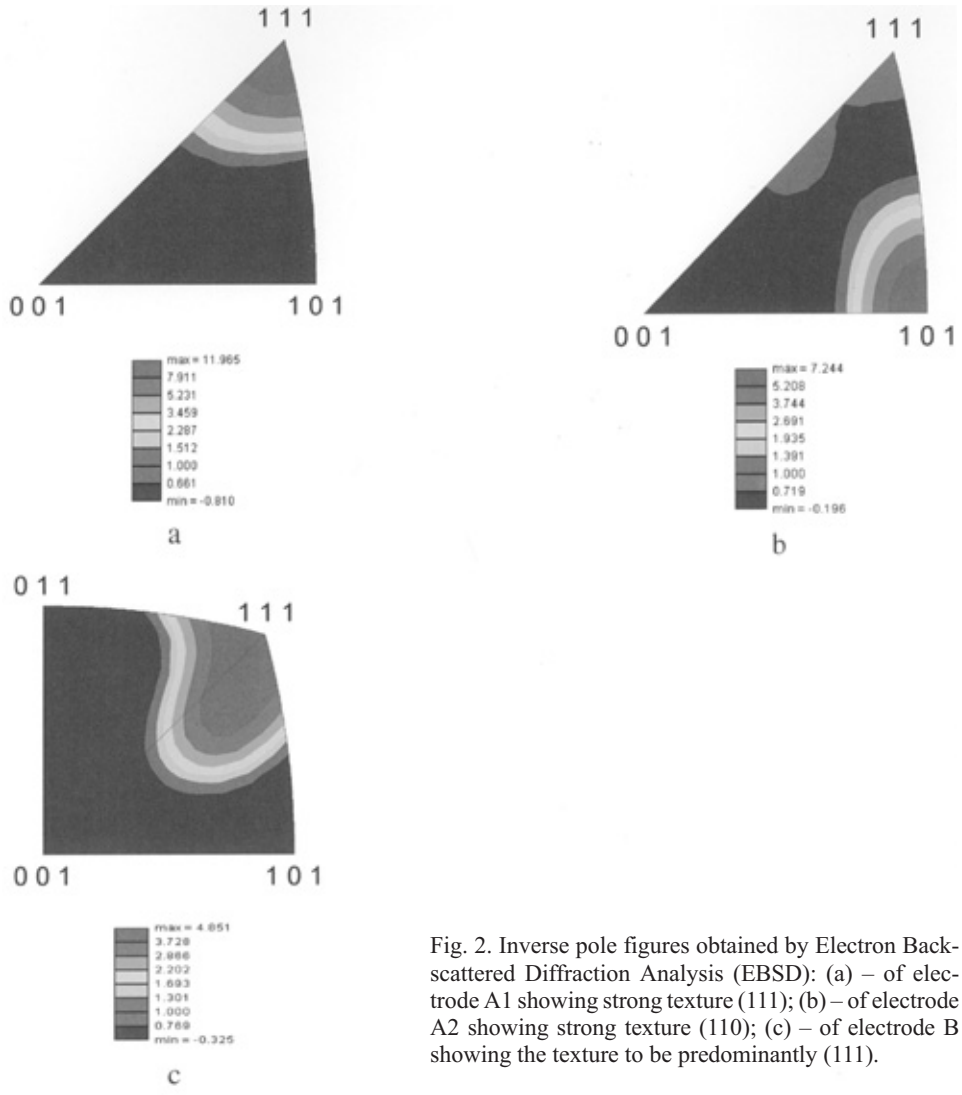

Fig. 2. Inverse pole figures obtained by Electron Backscattered Diffraction Analysis (EBSD): (a) – of electrode A1 showing strong texture (111); (b) – of electrode A2 showing strong texture (110); (c) – of electrode B showing the texture to be predominantly (111).

Electrode B. The texture of this electrode is shown in Fig. 2c, indicating a dominant (111) structure perpendicular to the electrode surface, which is due to the orientation of crystallites of the rolled chromium rod and elongation of crystallites in the (111) direction.

Electrode C. Texture analysis of this electrode was not performed but, from the literature,[13] it is known that electroplated chromium always has the (111) texture, except when large amounts of hydrogen were absorbed during the plating, when a hexagonal structure could be obtained. However, after two days, it transforms back to a bcc lattice. Namely, the hexagonal lattice corresoponds to CrH or CrH_2 hydrides. After desorption of hydrogen the bcc lattice is recovered. Due to

the time elapsed between the chromium plating of this sample and the electrochemical experiments in the present work it could be considered that the investigated surface was of preferentially oriented (111) crystallites.

Polarization measurements

Electrode A. The polarization curves presented in Fig. 3 are the results of five independent measurements with electrode A, *i.e.,* Merck, shown in Fig. 1a in the 0.1 M Na_2SO_4 + H_2SO_4 solution of pH 1. This diagram shows that the reproducibility of these measurements was very high, which is not often encountered in electrochemical kinetics measurement. The corrosion potential $E_{corr.2}$ was –0.715 V, estimated from the anodic and cathodic Tafel slopes $b_a = b_c = 0.120$ mV dec^{-1}, which corresponds to the values reported by Dražić and Popić[1] for the same electrode material.

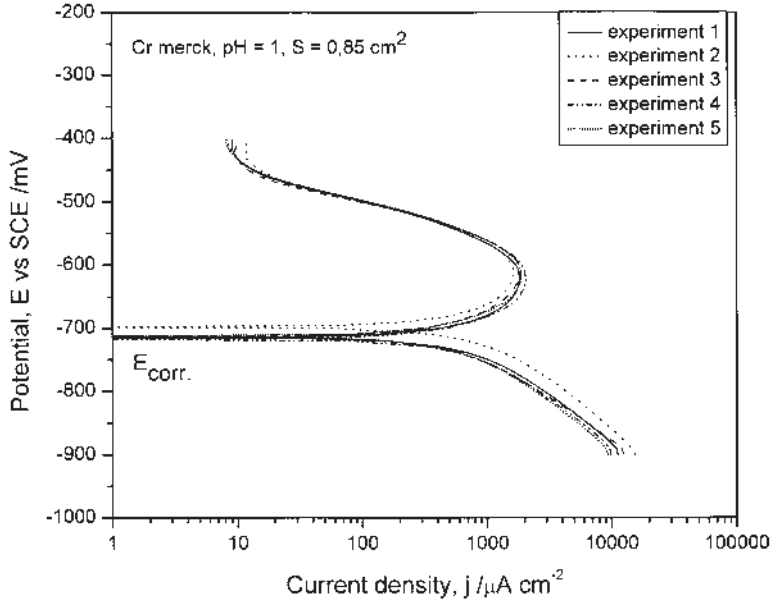

Fig. 3. Polarization curves for 5 independent experiments with the electrode A.

Electrode A1. The polarization curves for this part of the Merck electrode (A) are presented in Fig. 4. The open signs are related to A1 electrode. Also, the results of the analytical determination of the total concentration of dissolved Cr at the corrosion potential, expressed as the current density, is presented by the open squares. It is almost two times larger than the electrochemical corrosion determined by Tafel line extrapolation, indicating an additional corrosion process, most probably the chemical dissolution of chromium proposed by Kolotyrkin *et al.,*[9] involving the direct reaction of water molecules and hydronium ions with the metal. The passivation peak current density is 3 mA cm^{-2} somewhat larger than for the electrode A, presented in Fig. 3. The Tafel slopes, both anodic and cathodic, as well as

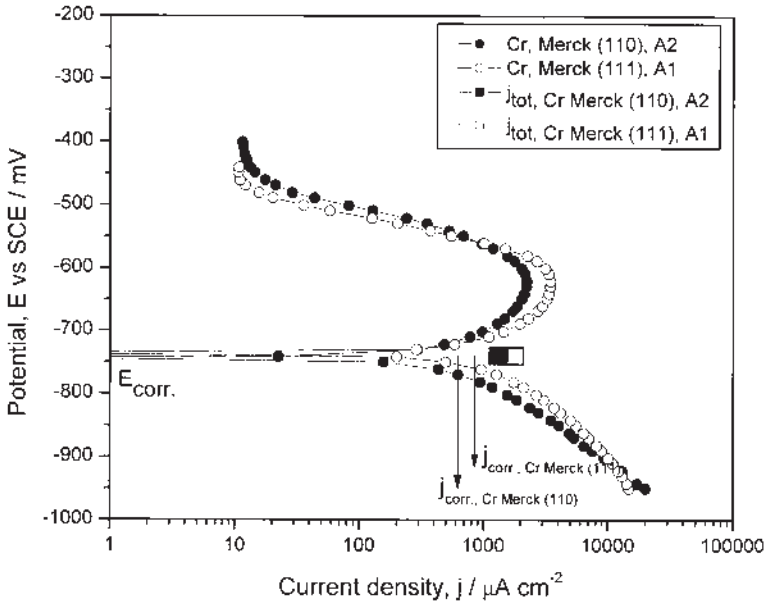

Fig. 4. Polarization curves for two grains of different orientations; A1 (111) and A2 (110) in electrode A. Analytically estimated corrosion current densities (*i.e.,* total) are marked with squares.

the corrosion potentials are approximately the same. Since, as shown before the structure of the A1 electrode is predominantly (111), which is the least packed face, it is to be expected that the dissolution of this plane would be faster than that of the well packed ones.

Electrode A2. The polarization curves for this electrode are also presented in Fig. 4 (filled signs), for easier comparison with electrode A1. Even though the basic shape of these curves is the same for both electrodes, the A2 electrode shows a somewhat smaller electrochemical activity, both for the cathodic and anodic reaction, which also produced a smaller corrosion current density. The passivation current peak was also smaller. However, the chemical reaction of Cr dissolution was also nearly the same as the electrochemical corrosion rate (the chemical dissolution rate is the difference between the total dissolution rate (filled square) and $j_{\mathrm{corr,Merck(110)}}$).

Electrode B. The four repeated independent experiments showed very good reproducibility, similar to that for electrode A, shown in Fig. 3. In order to economize on space, these diagrams are not shown here. One of these polarization diagrams is shown in Fig. 5, together with the polarization diagrams for electrodes A and C. This electrode also shows the appearance of the chemical reaction, together with the electrochemical corrosion. This is obvious from the position of the total dissolution rate (filled triangle) as compared to the corresponding electrochemical corrosion density. Corrosion potential is approximately the same as for electrodes A1 and A2, *i.e.,* ≈ -0.710 V.

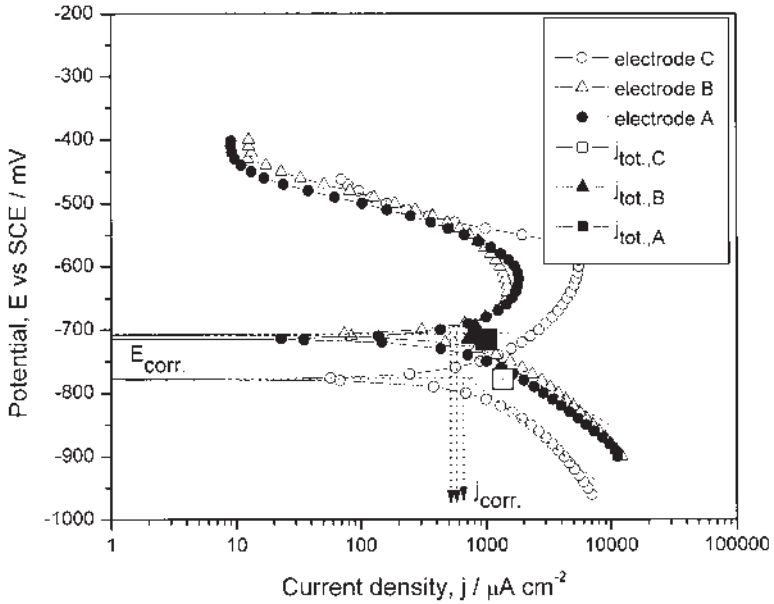

Fig. 5. Comparative presentation of the polarization curves for the electrodes A, B and C. Analytically estimated corrosion current densities (*i.e.,* total) are marked with squares and a triangle.

Electrode C. Five independent measurements were made with electrode C and they all showed very good reproducibility, similar to that for electrode A (Fig. 3). Therefore, as for electrode B, these results will be omitted in this paper. A typical polarization diagram for electrode C is also shown in Fig. 5 (open circles). This diagram is considerably different from those for electrodes A1, A2 and B. First, the corrosion potential of electrode C is more negative ($E_{corr.2} = -0.775$ V and the position of the anodic polarization curve shows an almost 4 times higher electrochemical activity, as compared to electrode A or B, while the cathodic hydrogen evolution was inhibited for the same ratio. This resulted in a change of the corrosion potential in the negative direction, as already mentioned, but without a serious effect on its corrosion current densities. The chemical dissolution rate determined from the total analysis of Cr (Fig. 5, open squares) showed that the rate is approximately the same as for the electrochemical corrosion.

Corrosion rates

As already shown in the previous polarization diagrams, the corrosion rates of all the electrodes determined by chemical analyses of the electrolyte were larger than the electrochemical corrosion rate determined from the extrapolation of the Tafel lines (Wagner and Traud).[5] In order to check the validity of the extrapolation method the electrochemical corrosion rates were also determined by the Stern–Geary[14] and electrochemical impedance spectroscopy methods.[15] The obtained parameters for the all the studied electrodes together with the corrosion rates

calculated from the analytical data, using an apparent valence $n = 2.12$[1] are given in Table I. The chemical corrosion rate was obtained by subtracting the electrochemical (Wagner–Traud) corrosion rate from the analytically obtained one.

TABLE I. Corrosion rates for the electrodes A1, A2, B and C obtained by different methods at 298 K

Electrode	Corrosion rate, j/mA cm^{-2}					Electrode capacitance μF cm^{-2}
	Wagner–Traud	Stern–Geary	EIS	Analytical	Chemical	
A	0.56	0.69	0.67	1.00	0.44	53±3
A1 (111)	0.98			1.58	0.60	
A2 (110)	0.75			1.10	0.31	
B	0.59	0.48	0.40	0.81	0.22	74.4±6
C	0.62	0.78	0.76	1.35	0.63	103±18

Effect of temperature

The temperature has a considerable effect on the corrosion rates, as shown elsewhere for the Merck electrode material (*i.e.,* electrode A).[3] In this work, similar measurements were carried out on electrode B. The results are presented in Fig. 6 for the electrochemical corrosion rates and total (analytical) corrosion rates as a function of temperature. It is interesting that the chemical dissolution rate (the difference between $j_{corr,an}$ and $j_{corr.el}$) increase faster than the electrochemical corrosion rate. At 353 K, they become 3 times faster than the electrochemical one, while at 293 K they are approximately equal (see Fig. 6).

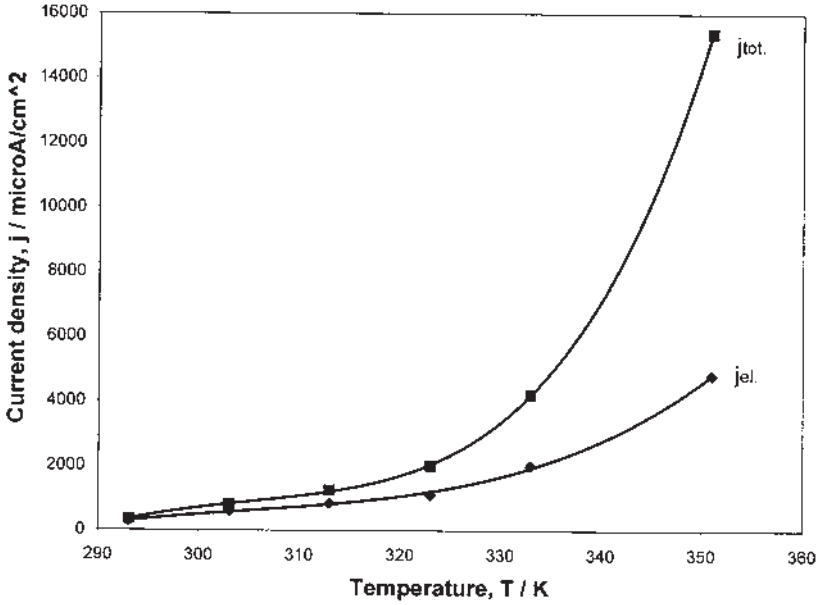

Fig. 6. Corrosion current densities determined analytically (*i.e.,* total) (squares) and electrochemically (diamonds) as a function of temperature.

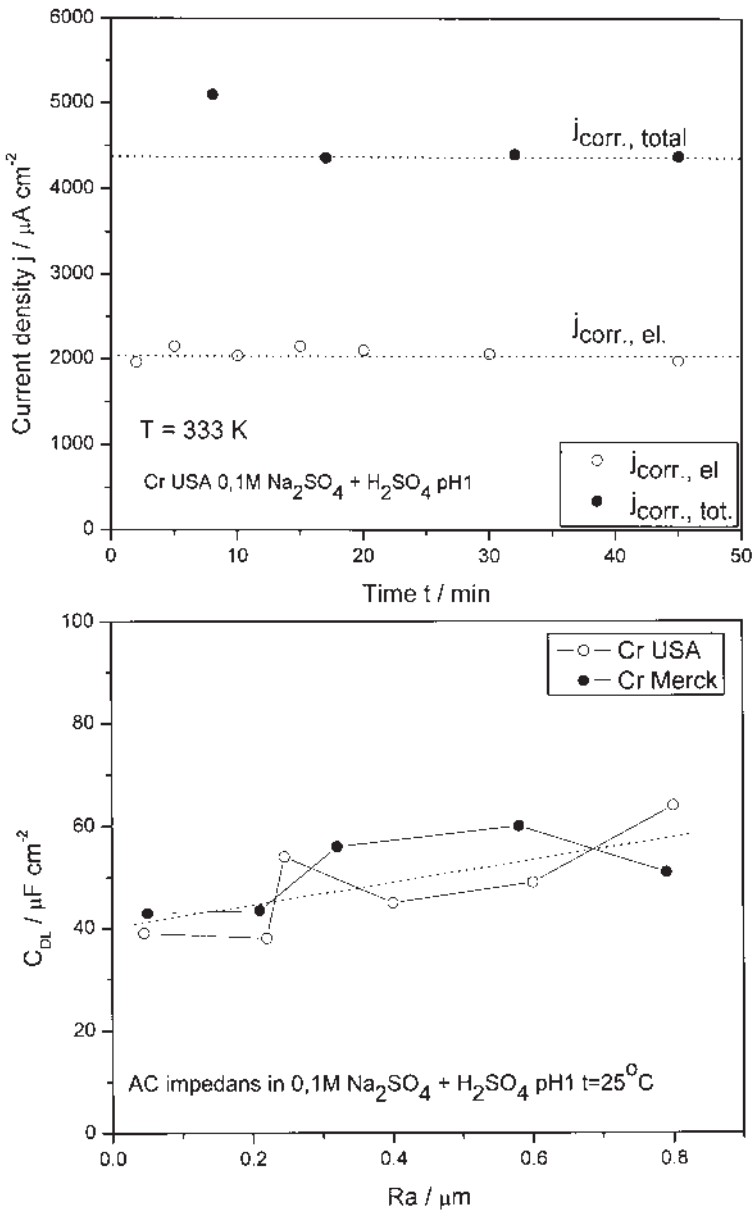

Fig. 7. (a) – Time dependence of the analytically (*i.e.*, total) and electrochemically determined Corrosion currents at 333 K: (b) – Dependence of the electrode capacitance on the average micro roughness (*i.e.,* coarseness).

There are some considerations that during corrosion the electrodes surface roughness increases and also that at higher corrosion rates (*e.g.*, at higher temperatures) the apparent current densities including the corrosion current densities do not correspond to the real surface area. If it is assumed that the electrode capaci-

tance is proportional to the surface these values can be a measure of the change of the real surface area. The values of the electrode capacitance obtained from the EIS measurements show that even though the macro roughness measured with a prophylometer changed with corrosion time, the electrode capacitance values did not change within the limits of experimental error. The same values were obtained for electrodes A and B.

Similarly, both corrosion rates (*i.e.,* the analytical and electrochemical) followed over time, as shown in Fig. 7a, remained practically unchanged during 60 min. These experiments were performed at 333 K in order to decrease the effects of experimental errors on the results. In other words, an increase of the macro roughening (coarsing) did not change the observed corrosion rates, which obviously depended only on the real surface roughness. Also, the electrode capacitances were constant as the macro roughness changed during a prolonged corrosion process (see Fig. 7b). Despić and Popov[16] in their analysis of the effect of surface roughening pointed out the difference between surface roughness and coarseness and the fact that there are situations when the real surface area remains the same even though the coarseness can change considerably. Of course, this is not always the case. The real surface roughness at the atomic level is usually estimated by comparing the electrode capacitance with the capacitance value of 18 μF cm^{-2}, which is a capacitance of the mercury electrode. Capacitances of 40–50 μF cm^{-2} are usually observed for solid corroding electrodes,[17] indicating a real surface roughness factor of about 2.5 for the Merck chromium and 5 for the electrochemically deposited chromium (electrode C). The factor 5 indicates that the coarseness of this electrode, as seen after some time of corrosion (Fig. 1c2), is responsible for this effect.

DICUSSION

The influence of the crystal orientation of chromium on its electrochemical behavior

The polarization curves obtained for the different electrodes were rather similar except for the electrode C, which behaved considerably different. Bearing in mind that the reproducibility of the measurements in electrochemical kinetics is not very high and might depend on a number of factors, or might be thought that the observed differences between the electrodes A, A1, A2 and B are within experimental error. However, repeated experiments with the same material 4–5 times, as shown for he electrode A in Fig. 3 as an example, clearly shows that the differences observed in the polarization curves for A1, A2 and B are much higher than the differences due to the bad reproducibility. Therefore, there is no other possibility than to conclude that the observed differences in the structures of the employed electrodes are at least one of the reasons for the observed differences (see Figs. 4 and 5).

The electrochemistry of the deposition and dissolution of single crystal metals is studied mostly in attempts to evaluate the mechanism of the electrocrystalliza-

tion processes. Works related to the dissolution of single crystals are scarce. Single crystals of nickel[18,19] and aluminium[20] were the subject of studies, while single crystal chromium was studied by Shcherbakova *et al.*[21] and Dobbelaar and de Wit.[22] Therefore almost all the literature related to single crystals is devoted to electrocrystallization.[23–25] It was shown, in particular in the case of Ag and Cu electrodeposition that the deposition mechanism might have two reaction paths; one by the direct deposition of a metal ion after its jump through the double layer and discharge reaction into the most stable position in the lattice, *e.g.,* kink sites and similar, and the second one by discharge onto a flat filled crystal face, with the subsequent surface diffusion of adatoms over the surface to the most stable position in the kink sites and corners, *i.e.,* so-called half-crystal positions. The presence of the dislocations at the surface does not change this picture except that the density of dislocations, either in a linear or spiral form, can change the surface diffusion paths. In a classical work of Bockris and Conway,[23] it was shown that energetically it is easier to have surface diffusion and adatom formation during the deposition process than to have a direct jump into a stable half-crystal position. This difference does not mean that there are no direct jump steps, but that the deposition occurs predominantly by the surface adatom diffusion mechanism. Even though there are practically no experimental results of the electrochemical dissolution rates of single crystal metals, it is assumed that the dissolution mechanism is just the reversal of the deposition one, *i.e.*, that it passes through similar dissolution steps, involving adatoms, their surface diffusion and final jump through the double layer. All these theories were developed after studying the deposition on the copper and silver crystals which have a fcc crystal lattice and where the (111) face is the closed packed face. Their idea is that during the dissolution all higher index faces dissolves faster and that after some time the only remaining face is the closed packed one, *i.e.,* the (111). The reasoning is simple; this is the surface structure with the highest interaction of an atom with the neighboring atoms and therefore with the largest activation energy for dissolution.

With chromium which has a bcc structure the same reasoning for the energetic situation is different. Figure 8 depicts the surface structures of of three different

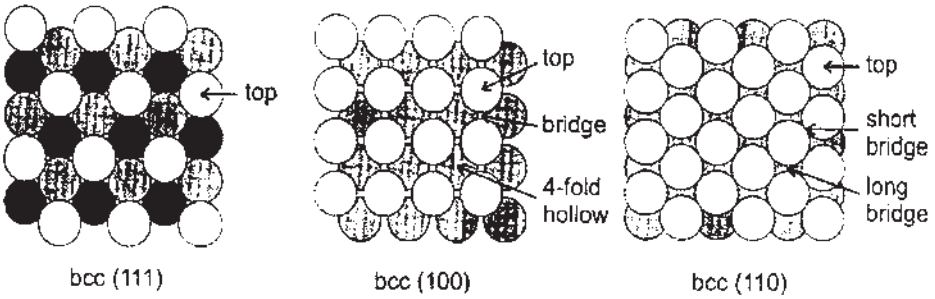

Fig. 8. Model presentation of the surface structures for three different low density index planes of the bcc crystal lattice.

faces of chromium, showing that the (111) face has atoms with the least number of interactions with their neighbors. Therefore, it can be expected that the (111) face will dissolve more readily than all the others. It seems that this is exactly the reason why the A1 electrode (111) dissolves faster than the electrode A2 (110) (see Fig. 4). This can also be seen on the SEM picture of boundary region between the A1 and A2 electrodes after the corrosion presented in Fig. 1 a2. This is in agreement with our finding in experiments in an AFM studies[4] of the Merck electrode surface, where the A1 surface was found to dissolve faster than the other surface. This is also in accord with the results of Shcherbakova *et al.*[21] who found that the dissolution rates increased in the order (110) < (111) < (100). However, it should be pointed out here that in that paper,[4] which was based on X-ray Laue analysis, it was erroneously reported that electrode A1 was amorphous. It appears that the fine substructure of the dominantly(111) orientation, as observed in the present study by a better technique, could not be detected by the previously used Laue technique.

However, the much higher anodic dissolution rates of the electrolytically deposited Cr cannot be explained by its crystallographic orientation (as mentioned before, practically all data in the literature agree that this deposit is textured and generally has (111) orientation.[13] The difference in the anodic activity of electrodes B and C is considerable, even though the crystallographic orientations are practically the same, or similar. This higher anodic activity of electrode C could be explained either by the much higher concentration of surface dislocations, often observed in cathodically deposited metals,[24] or by the very large surface roughness and large number of cracks in the deposit, as observed in the microphotograph of electrode C after corrosion (see Fig. 1c2), or both. More work is needed to clarify this point. It is also interesting, that the hydrogen evolution rates at electrode C are inhibited to the same extent as the anodic reactions are accelerated so that the corrosion potential, which is the intersection potential of the cathodic and anodic Tafel lines is practically the same for electrodes B and C, giving the impression that there are no differences between them.

Chemical dissolution of chromium

Systematic results of the chemical analyses of sulfuric acid solutions after leaving of chromium electrodes in them for some time show that all the chromium electrodes dissolved about two times faster than would correspond to the electrochemical corrosion of each electrode. This fact was already experimentally verified in some of our previous works[13] and also much earlier by Kolotyrkin and Florianovich.[7] From the experimental data presented in this work, it seems that the crystallogarphic orientation of the chromium influence the rate of its chemical dissolution in the same way as by electrochemical dissolution. As shown elsewhere[2] this chemical process can be represented by

$$Cr + H_2O \leftrightarrow CrOH_{ads} + H \quad (1)$$

$$CrOH_{ads} + H^+ \rightarrow Cr^{2+} + H + OH^- \quad (2)$$

$$2H \rightarrow H_2 \quad (3)$$

$$Cr + H_2O + H^+ = Cr^{2+} + H_2 + OH^- \quad (4)$$

in which there are no electrochemical reactions, chromium is chemically dissolved (or corroded) with the simultaneous evolution of hydrogen (the overall reaction (4)), and most importantly, these reactions are independent of the electrode potential. They can be accelerated only by a decrease of the solution pH and an increase of temperature. It should be noted here, that according to the results presented elsewhere[3] the chemical dissolution rate increases faster with increasing temperature than the electrochemical dissolution rate. Therefore, one should take into consideration that when corrosion rates of chromium are determined by electrochemical methods at elevated temperatures, the real corrosion rates might be several times faster than the electrochemically determined ones. Also, chemical dissolution might be important in the processes involved in stress corrosion cracking, especially at the elevated temperatures, since the electrochemical potentials at the crack tips are of no importance whatsoever.

CONCLUSION

Studies of the electrochemical behavior of three different metallic chromium samples of different origin and pretreatment showed that they have some properties of the single crystal structures of the (111) or (110) orientation, which in sulfuric acid solution (pH 1) have a somewhat different electrochemical activity both for the anodic dissolution and cathodic hydrogen evolution reactions. The (111) surface dissolves faster and hydrogen evolves faster on it, than the (110) face. Electrolytically deposited chromium, which is assumed on the basis of literature data to have the (111) structure, dissolves much faster than the single crystal (111) face, but the hydrogen evolution reaction is inhibited by the same degree. Possible reasons for this could be the very different coarseness of these surfaces. All the materials showed that dissolution, and corrosion, occurs through two parallel processes. The first one is the potential dependent electrochemical dissolution reaction, while the second one is the potential independent chemical reaction of chromium with water molecules. Both processes proceed at approximately same rate at the room temperature, while at 333 K, the chemical rate is *ca*. 3 times faster than the electrochemical one. The importance of this finding in relation to the processes involved in stress corrosion cracking is pointed out.

Acknowledgements: This work was financially supported by the Ministry of Science and Environmental Protection of the Republic of Serbia (Grant No. 142061), and the Serbian Academy of Sciences and Arts, Belgrade (Project F-7).

ИЗВОД

УТИЦАЈ СТРУКТУРЕ МЕТАЛНОГ ХРОМА НА ЊЕГОВО ЕЛЕКТРОХЕМИЈСКО ПОНАШАЊЕ

БОРЕ ЈЕГДИЋ[1], ДРАГУТИН М. ДРАЖИЋ[2], ЈОВАН П. ПОПИЋ[2] и ВЕЛИМИР РАДМИЛОВИЋ[3]

[1]Институт за хемијске изворе струје, Батајнички друм бб, 11070 Београд-Земун, [2]Институт за хемију, технологију и металургију-Центар за електрохемију, Његошева 12, п. пр. 473, 11001 Београд и [3]Lawrence Berkeley National Laboratories, University of California, Berkeley, CA, USA

Проучавано је електрохемијско растварање хрома у воденим растворима сумпорне киселине (pH 1) са електродама од хрома различите кристалографске структуре. Примењена је спора потенциодинамичка метода у деаерираним растворима (уз провођење азота) на 25 °C, а јони Cr(III) у раствору после одређеног времена корозије одређивани су атомском апсорпционом спектроскопијом. У експериментима су употребљена три електродна материјала са доминантним кристалним структурама које подсећају на моно кристалне (тј. 111 и 110), а што је потврђено EBSD методом. Нађено је да је структура (111) електрохемијски активнија (и анодно и катодно) од структуре (110). Међутим, електролитички исталожен Cr из стандардног купатила за хромирање, а који на основу литературних података има структуру (111) био је око 4 пута активнији у анодној реакцији и исто толико мање активан за катодну реакцију издвајања водоника. Аналитички одређиване концентрације Cr(III) јона у раствору после одређеног времена спонтане корозије показивале су два пута веће концентрације него што би се очекивало на основу брзине електрохемијске корозије, одређиваних методама Wagner–Traud, Stern–Geary и електрохемијском импедансном спектроскопијом. Ово је објашњено једновременим одигравањем и електрохемијске реакције и хемиске реакције директног реаговања металног Cr са молекулима воде, по механизму предложеном од Колотиркина и сарадника.

(Примљено 20. фебруара 2007)

REFERENCES

1. D. M. Dražić, J. P. Popić, *Corrosion* **60** (2004) 297
2. J. P. Popić, D. M. Dražić, *Electrochim. Acta* **49** (2004) 4877
3. J. P. Popić, D. M. Dražić, *J. Serb. Chem. Soc.* **68** (2003) 871
4. D. M. Dražić, J. P. Popić, B. Jegdić, D. Vasiljević-Radović, *J. Serb.Chem. Soc.* **69** (2004) 1099
5. C. Wagner, W. Traud, *Z. Electrochem.* **44** (1938) 391
6. G. M. Florianovich, Ya. M. Kolotyrkin, *Dokl. Akad. Nauk SSSR* **157** (1964) 422
7. Ya. M. Kolotyrkin, G. M. Florianovich, *Zashch. Metal.* **1** (1965) 7
8. Ya. M. Kolotyrkin, G. M. Florianovich, *Elektrokhimiya* **9** (1973) 988
9. G. M. Florianovich, Ya. M. Kolotyrkin, L. A. Sokolova, *Proc. 3rd Int. Congress Metallic Corrosion,* Moscow, 1966, p. 190
10. Ya. M. Kolotyrkin, G. M. Florianovich, *Z. Phys. Chem.* **231** (1966) 145
11. V. M. Knyazheva, Ya. M. Kolotyrkin, A. A. Kruzhovskaya, *Zashch. Metal.* **6** (1970) 265
12. Ya. M. Kolotyrkin G. M. Florianovich, *Glasnik Hem. Društva Beograd* **48** (1983) S125
13. *Modern Electroplating,* F. A. Lowentheim, Ed., Wiley, New York, 1974, pp. 121, 122
14. M. Stern, A. L. Geary, *J. Electrochem. Soc.* **104** (1957) 56
15. F. Mansfeld, in *Advances in Corrosion Science and Technology*, Vol. 6, M. G. Fontana, R. W. Staehle, Eds, Plenum Press, New York, 1976

16. A. R. Despić, K. Popov, in *Modern Aspects of Electrochemistry,* B. E. Conway, J. O'M. Bockris, Eds., Plenum Press, New York, 1972, pp. 199, 203
17. J. O'M. Bockris, D. M. Dražić, A. R. Despić, *Electrochim. Acta* **4** (1961) 325
18. O. M. Magnussen, J. Scherer, B. M. Ocko, R. J. Behm, *J. Phys. Chem. B,* **104** (2000) 1222
19. V. V. Konovalov, G. Zangrari, R. M. Metzger, *Chemistry of Materials* **11** (1999) 1949
20. L. N, Yagupolskaya, *Zashch. Metal.* **6** (1970) 614
21. L. G. Shcherbakova, L. N. Yagupolskaya, N. A. Krapivko, *Elektrokhimiya* **24** (1988) 1113
22. J. A. I. Dobbelaar,J. H. W. de Wit, *J. Electrochem. Soc.* **139** (1992) 716
23. B. E, Conway, J. O'M. Bockris, *Proc. Roy. Soc.* **A248** (1967) 394
24. J. O'M. Bockris, A. Damjanović, in *Modern Aspects of Electrochemistry,* No. 3, J. O'M. Bockris, B. E. Conway, Eds., Butterworth, London, 1966, pp. 261–273
25. E. Budevski, in *Comprehensive Treatise of Electrochemistry,* Vol. 7a, B. E. Conway, J. O'M. Bockris, E. Yeager, S. U. M. Khan, R. E. White, Eds., Plenum Press, New York, 1983.